Resonant scattering of phonons in the quasi-one-dimensional spin-chain compounds AB_2O_6 (A = Ni, Co; B = Sb, Ta)

N. Prasai,[1] A. B. Christian,[2] J. J. Neumeier,[2] and J. L. Cohn[1]
[1]*Department of Physics, University of Miami, Coral Gables, Florida 33124, USA*
[2]*Department of Physics, Montana State University, Bozeman, Montana 59717, USA*

(Received 30 May 2018; revised manuscript received 3 October 2018; published 30 October 2018)

We report measurements of thermal conductivity (κ) on single crystals of the quasi-one-dimensional antiferromagnetic spin-chain compounds AB_2O_6 (A = Ni, Co; B = Sb, Ta) in the temperature range $5 \leqslant T \leqslant 300$ K. We find that κ for all crystallographic directions is substantially suppressed in the Ta compounds in comparison to those of the Sb compounds despite their very similar magnetic and crystallographic structures. The data are well described by resonant scattering of phonons from two-level systems, with energy splittings of ∼100–150 K and scattering strength an order of magnitude greater in the Ta compounds. We distinguish the effects of phonon-spin interactions from those related to changes in the low-energy phonon spectra caused by the different B-site ions.

DOI: 10.1103/PhysRevB.98.134449

I. INTRODUCTION

The predominance of spin-phonon damping in low-dimensional spin systems for which there is significant overlap in the spin and phonon excitation spectra ($J \leqslant \Theta$) makes them particularly interesting for study. Thermal conductivity is a sensitive probe of these interactions through the scattering of long wavelength, heat-carrying phonons via magnetic excitations as observed in the spin-Peierls compound $CuGeO_3$ [1], quasi-two-dimensional (2D) spin system $SrCu_2(BO_3)_2$ [2], and spin-$\frac{1}{2}$ chain [3] and ladder [4] compounds.

The AB_2O_6 (A = Co, Ni; B = Sb, Ta) compounds form a class of quasi-one-dimensional AF chain compounds with spin-1 (Ni) and spin-3/2 (Co). Very similar to the spin-$\frac{1}{2}$ $CuSb_2O_6$ analog [3,5–10], these compounds are characterized by the development of short-range, quasi-one-dimensional (q1D) magnetic order at temperatures far above their long-range, three-dimensional (3D) ordering temperatures T_N = 13.45 K for $CoSb_2O_6$ [5,11], 6.6 K for $CoTa_2O_6$ [12], 6.7 K for $NiSb_2O_6$ [9], and 10.5 K for $NiTa_2O_6$ [12,13]. They have trirutile crystal structure with tetragonal unit cell ($P4_2/mnm$ space group), the transition metal ions residing in an octahedral environment. The dominant exchange pathways defining their AF chains [14] [A-O-O-A] are along the [110] and [1$\bar{1}$0] directions, with their orientation rotating by 90° between neighboring layers along the crystallographic c axis, thereby giving rise to a two-sublattice description of the magnetic structure [5–8]. Long-range ordering at T_N in these compounds can be viewed as a 1D to 3D transition realized through alignment of q1D regions and further alignment of stray magnetic moments [5,6], with differing magnetic unit cells [15] and values for T_N reflecting variations in the weak interchain exchange coupling.

The spin correlations for half-integer and integer (Haldane) spin chains are qualitatively different [16,17], with the latter decaying exponentially due to the presence of a gap in the excitation spectrum. This difference might manifest itself in spin-phonon coupling as probed through thermal conductivity measurements. Our prior study [3] of κ in $CuSb_2O_6$ revealed a substantially suppressed thermal conductivity in comparison to the nonmagnetic analog compound $ZnSb_2O_6$, and the additional scattering was attributed to resonant phonon scattering from two-level systems associated with the short-ranged spin order. The Ni and Co compounds, as we report here, show a more complex behavior: compounds with Sb on the B site exhibit negligible or relatively weak resonant phonon scattering and those with Ta show dramatically enhanced resonant scattering. We model the lattice thermal conductivities to extract the resonance energies and, by comparing the approximate phonon and magnetic excitation spectra, attempt to distinguish effects of phonon-spin coupling from changes in the phonon spectrum associated with the Ta ion. We conclude that the strong resonant scattering in the Ta compounds is not due to excitations of the spin system, but rather a consequence of interaction between a low-lying optic-mode phonon with heat-carrying transverse acoustic modes.

II. EXPERIMENT

Single crystals studied in this work were grown by chemical vapor transport (Sb compounds) and optical floating-zone method (Ta compounds) as described in detail elsewhere [5–7,9]. Specimens were oriented by x-ray diffraction for heat flow along the principal crystallographic axes and along the chains ([110]), and polished into thin parallelopipeds with typical dimensions $1.5 \times 0.18 \times 0.18$ mm^3. A standard steady-state method was employed for measuring thermal conductivity, with temperature gradient produced by a chip heater and monitored by a 25-μm-diameter chromel-constantan differential thermocouple. In most cases for each of the four compounds, at least two specimens were measured with heat flow along each direction, confirming the reproducibility of $\kappa(T)$ within uncertainties (≃15% dictated by the geometric factor). Corrections for radiation losses, which would reduce κ by 10%–15% at $T \geqslant 200$ K, have not been applied.

 ©2018 American Physical Society

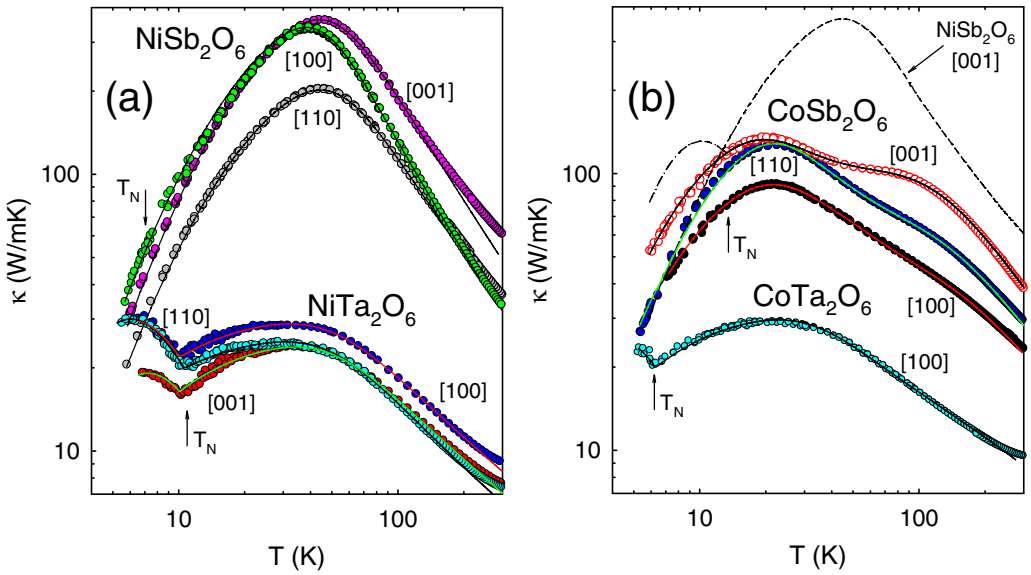

FIG. 1. Thermal conductivity vs temperature along several direction for (a) $NiSb_2O_6$, $NiTa_2O_6$ and (b) $CoSb_2O_6$, $CoTa_2O_6$. Vertical arrows indicate T_N for each compound. Solid curves are computed from the model described in the text. The dash-dotted curve in (b) represents the fit to the $CoSb_2O_6$ [001] sample with resonant scattering decay at $T < T_N$ (see text).

III. RESULTS AND ANALYSIS

Figure 1 shows $\kappa(T)$ for the four compounds along different crystallographic directions. Any spin contribution to κ would tend to enhance κ within the *ab* plane—the absence of such anisotropy indicates that κ is predominantly phononic. The key observations are: (1) κ is substantially suppressed in the Ta-containing compounds relative to those with Sb, (2) the Ta compounds exhibit a sharp upturn in $\kappa(T)$ for $T \leqslant T_N$ (vertical arrows), whereas no discernible influence of T_N is detected in the Sb compounds, and (3) the $CoSb_2O_6$ compounds have $\kappa(T)$ suppressed relative to $NiSb_2O_6$ (the latter is reproduced by the dashed curve in the right panel for comparison)—the shoulder or dip in the $CoSb_2O_6$ $\kappa(T)$ in the range 50–60 K is typical of resonant phonon scattering, i.e., an energy-dependent scattering rate characterized by a maximum at a particular phonon energy. As we now discuss, this feature in $\kappa(T)$ for $CoSb_2O_6$ and the more dramatic suppression of $\kappa(T)$ for the Ta compounds are modeled well by resonant scattering rates with energy scales 100–150 K. Observation (2) above indicates the strong scattering characterizing the Ta compounds is coupled to short-range quasi-one-dimensional AF order, developing at $T \gg T_N$, that is rapidly diminished with the onset of long-range order at $T < T_N$. That this resonant scattering occurs for all transport directions indicates that, insofar as spin excitations are involved, they are likely localized since otherwise the constraints on momentum conservation within the *ab* plane would yield anisotropy in the scattering rate for phonons.

Callaway model [18] fitting to the data was employed to quantify the resonant phonon scattering. $\kappa(T)$ was computed as

$$\kappa_L = \frac{k_B}{2\pi^2 v}\left(\frac{k_B T}{\hbar}\right)^3 \int_0^{\Theta/T} \frac{x^4 e^x}{(e^x-1)^2}\tau(\omega,T)dx,$$

where $x = \hbar\omega/k_B T$, ω is the phonon angular frequency, and $\tau(\omega, T)$ is the phonon relaxation time. The Debye temperature is computed from the average phonon velocity (v) as $\Theta = (\hbar v/k_B)(6\pi^2 n/V)^{1/3}$, where n is the number density of atoms ($n = 18$) and $V \simeq 200$ Å^3 is the unit cell volume (2 formula units).

We first fitted the $\kappa(T)$ data for $NiSb_2O_6$ by incorporating phonon scattering terms representing boundaries, dislocations, point defects, and Umklapp processes, respectively:

$$\tau(\omega,T)^{-1} = \frac{v}{\ell_0} + A\omega + B\omega^4 + C\omega^2 T \exp\left(-\frac{\Theta}{bT}\right),$$

where $\ell_0 \equiv 2\sqrt{a/\pi}$ (a is the specimen cross-sectional area), and A, B, C, and b are fitting parameters. Since only the Sb and Ta masses differ significantly, the acoustic phonon dispersions are expected to be quite similar for the Sb compounds and separately for the Ta compounds. By exploring the parameter space, sound velocities that successfully fit each series of compounds were determined to be $v = 3.3$ km/s (Sb) and 2.4 km/s (Ta), corresponding to Debye temperatures $\Theta = 440$ K (Sb) and 320 K (Ta). Following observations [19] that the effective temperature scale for Umklapp scattering in multiatom unit cells scales as $\Theta/n^{1/3}$, parameter b was fixed to be $18^{1/3} = 2.6$ for all compounds.

Fitting to data for $CoSb_2O_6$ and the Ta compounds required an additional resonant scattering term appropriate for a two-level system [20,21],

$$\tau_{\rm res}^{-1}(\omega,T) = R\frac{\omega^4}{\left(\omega^2-\omega_0^2\right)^2}[1 - c\tanh^2(\hbar\omega_0/2k_B T)],$$

where R is the scattering strength, ω_0 is the resonance frequency, and c is the concentration (per site) of two-level systems.

To model the upturn in $\kappa(T)$ for the Ta compounds at $T < T_N$ we added an empirical factor $(T/T_N)^3$ in the resonant

TABLE I. Fitting parameters for $\kappa(T)$ data. The resonance scattering parameters in parentheses for the Ta compounds were determined using a modified Callaway model using a dispersing phonon (see text). Values for the intrachain exchange constant (J) were determined from fits to the magnetic susceptibility [6,7,9,13,27].

Specimen	ℓ_0 (mm)	A (10^{-5})	B (10^{-44} s^3)	C (10^{-18} s K^{-1})	b	Θ (K)	R (10^{11} s^3)	$\hbar\omega_0/k_B$ (K)	c	J (K)
NiSb [100]	0.23	1.49	5.46	1.87	2.6	440	0			26
NiSb [110]	0.16	2.75	10.0	1.58	2.6	440	0			26
NiSb [001]	0.14	1.84	4.20	1.14	2.6	440	0			26
NiTa [100]	0.24	1.38	0	0.88	2.6	320	19.2 (3.60)	160 (120)	0.44 (0.37)	18.9
NiTa [110]	0.33	1.49	0	1.23	2.6	320	24.0 (5.30)	160 (120)	0.37 (0.33)	18.9
NiTa [001]	0.18	3.75	0	1.05	2.6	320	29.2 (6.50)	175 (135)	0.51 (0.42)	18.9
CoSb [100]	0.22	0.99	9.56	1.64	2.6	440	0.36	95	0.85	10.6
CoSb [110]	0.14	1.11	4.44	1.46	2.6	440	0.29	101	0.92	10.6
CoSb [001]	0.18	0.14	2.39	1.17	2.6	440	0.17	85	0.82	10.6
CoTa [100]	0.18	0	0	1.72	2.6	320	5.30 (1.60)	108 (90)	0.48 (0.43)	6.1
CuSb [100]	0.26	1.53	2.39	12.6	2.6	440	7.50	74	0.90	97

scattering rates to simulate the rapid decay of this scattering in the long-range AF ordered state. Examples of the fitting are shown by the solid curves in Fig. 1. Modeling this upturn provides an extra constraint on the strength of the resonant scattering and solidifies the connection between the resonant scattering and short-range spin order. It is noteworthy that no such feature is observed for $CoSb_2O_6$—the dash-dotted curve in Fig. 1(b) represents the effect, in fitting to the [001] specimen, that the same $(T/T_N)^3$ decay of resonant scattering would predict.

Parameter values for fits to all specimens are listed in Table I. The values for A, B, and C are similar to those employed for the CuSb and ZnSb compounds [3] and other complex oxides [22]. For the Ta compounds the resonant scattering predominates throughout most of the temperature range, so the fitting is insensitive to the point-defect scattering term (B). To compare to the present work we also include in Table I new fitting parameters for the CuSb data since Ref. [3] employed a different form for $\tau_{res}^{-1}(\omega, T)$. Note that the concentrations of resonant scatterers for CoSb and CuSb ($c \sim 0.8$–0.9) are about twice the values employed for the Ta compounds. Along with their different behaviors at $T < T_N$, these observations suggest that the resonant scattering in the Sb and Ta compounds may arise from different mechanisms, a possibility we discuss further below.

The use of dispersionless phonons in the Callaway model overestimates the thermal conductivity at temperatures for which the dominant phonons in the κ integral have energies exceeding those of the actual acoustic spectrum at the Brillouin zone boundary. Based on the measured phonon dispersions of rutile [23,24] we anticipate the energies of the transverse acoustic modes in the present compounds [25] to be near ~12–16 meV, close to the fitted values of $\hbar\omega_0$ for the NiTa specimens, thus raising a question as to the sensitivity of the latter to this aspect of the modeling. To assess this uncertainty, we refitted the data for the Ta compounds employing a dispersive phonon ($\propto \sin q$ with $v = 2.8$ km/s, see Fig. 2) within a modified Callaway formalism [26]. The resulting resonance energies are also included in Table I in parentheses, with the difference providing an estimate of uncertainties.

We also note that, though the NiSb data was modeled successfully without a resonant scattering term, the presence of weak resonant scattering with energy scale similar to that of NiTa cannot be excluded given that such a term can mimic the effects of the modest defect scattering terms employed in the fittings shown in Fig. 1.

IV. DISCUSSION AND CONCLUSIONS

As noted above, a mechanism for the phonon resonant scattering that involves excitation of the spin system likely involves nondispersing modes, given the apparent insensitivity of the scattering to the transport direction. Such a mechanism, invoked for a variety of low-dimensional spin systems [2,4,31,32], involves phonon-induced excitation of the magnetic system (with energy $\hbar\omega_0$) and subsequent

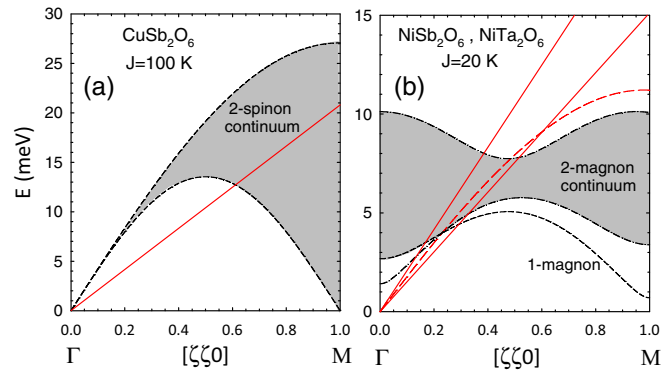

FIG. 2. Approximate phonon and spin excitation spectra of the compounds under study for momentum along the magnetic chains ($\zeta = qa/\pi$). The Debye phonons (solid lines) and dispersing phonon [long dashed curve in (b)] have velocities 3.3, 2.4, and 2.8 km/s, respectively, as employed in the $\kappa(T)$ fitting (see text). The two-spinon continuum for the $S = 1/2$ compound [shaded region in (a)] is bounded from below and above by dashed curves representing [28] $(\pi J/2)|\sin q|$ (the single-spinon dispersion) and $\pi J|\sin(q/2)|$, respectively. The single-magnon dispersion for the Ni $S = 1$ chain compounds is represented by [29] $\sqrt{\Delta^2 + v^2\sin^2(q) + \alpha^2\cos^2(q/2)}$ with Haldane gap $\Delta = 0.41J$, $v = 2.7J$, and $\alpha = 1.5J$ [dashed curve in (b)]. The boundaries of the noninteracting two-magnon continuum [shaded region in (b)] are shown by the dashed-dotted curves [30].

deexcitation that preserves total spin—effectively a strongly ω-dependent elastic scattering of phonons with random direction of the initial and final phonon momenta. For example, for systems of dimerized spins [2,4,31] phonons may induce transitions between singlet (ground) and triplet (excited) states of spin dimers.

Dimerization is plausible in the $S = 3/2$ Co compounds and was assumed in modeling their susceptibilities with an Ising model [6,8]. However, the resonance energies $\hbar\omega_0/k_B \sim 100$ K inferred from the κ analysis are equal to or twice as large as the energy difference between the lowest and highest energies for isolated dimers ($9J$) for CoSb and CoTa, respectively.

For the Cu and Ni compounds we consider fundamental excitations of the spin chains, comprising two-particle continua of spinons ($S = 1/2$) or magnons ($S = 1$), and their possible overlap in momentum and energy with the phonon spectrum [32,33], to look for potential resonant interaction. Figure 2 shows an approximate comparison of this sort for the phonons employed in the modeling and the spectra for isotropic Heisenberg chains.

For the $S = 1/2$ Cu compound [Fig. 2(a)] the constraints of momentum and energy conservation appear to allow for an acoustic phonon and spinon, with energies corresponding to $\hbar\omega_0 \sim 6.5$ meV, to combine and form a nondispersing spinon excitation near $q = \pi/2$. Such a process might be a candidate for resonant scattering, though the phase space for such processes would appear to be modest. For the $S = 1$ NiTa compound [Fig. 2(b)], the resonance at ~12.5 meV would appear to exceed the energy of the two-magnon continuum. Furthermore, the dominant spectral weight of Haldane chains occurs near the single-magnon dispersion at the lower boundary of the two-magnon continuum. These observations demonstrate that a mechanism for the resonant scattering relying on direct excitation of the different spin systems is elusive.

An alternative mechanism for resonant scattering involves the interaction of a low-lying optical phonon mode with transverse acoustic phonons, with the former shifted lower in energy in the Ta compounds due to the larger mass ($M_{\mathrm{Ta}}/M_{\mathrm{Sb}} \sim 1.5$) and weaker (less covalent) Ta-O bonds. This scenario is motivated by observations that Raman-active phonons involving motions of the B-site-oxygen octahedra are substantially lowered in frequency (by 15%–20%) in the Ta compounds compared to their Sb counterparts [34]. Such a shift would cause the optic phonon to hybridize with a transverse acoustic branch, the avoided crossing effectively opening a gap in the acoustic phonon dispersion (Fig. 3).

As for coupling to the spin system, Raman scattering studies of the CuSb and CoSb compounds [35] and other antiferromagnets [36,37] demonstrate that spin fluctuations renormalize optical phonon energies at temperatures well above T_N and when long-range order is established at

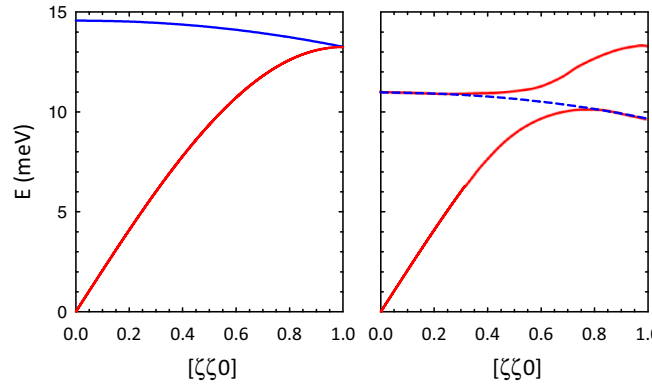

FIG. 3. Schematic of a transverse acoustic phonon and lowest-lying optic mode phonon in AB_2O_6. The left (right) panels depict the proposed spectra for the Sb (Ta) compounds, with the optic mode, lowered in energy by the larger mass and weaker bonding of Ta, hybridizing with the acoustic mode and opening a gap responsible for strong resonant scattering.

$T < T_N$. Similar effects for the optical phonon mode involved in the hypothesized crossing mechanism proposed for the Ta compounds could result in the upturn observed in κ at $T \leqslant T_N$, e.g., due to a shift in the energy of or narrowing in the induced gap in the transverse acoustic branch. The absence of such behavior in the Sb compounds suggests that the mechanisms for resonant scattering in the Sb and Ta compounds differ. That CuSb and CoSb exhibit resonant phonon scattering, whereas NiSb does not suggests a possible connection to spin (half integer vs integer). Efforts to further investigate these ideas would benefit from both theoretical and experimental determinations of the lattice dynamics for these interesting compounds.

In conclusion, the lattice thermal conductivities of the AB_2O_6 (A = Ni, Co; B = Sb, Ta) compounds are characterized by resonant scattering of phonons that is substantially enhanced in the Ta compounds independent of the A-site ion (spin). We hypothesize that this difference has its origin in a substantially lower optic-mode phonon energy in the Ta compounds that overlaps with and opens a gap in an acoustic phonon dispersion. Coupling of this optic mode to the spin systems is evidenced as a rapid decay of the resonant scattering at $T \leqslant T_N$. Weaker resonant scattering observed in $\kappa(T)$ for $CoSb_2O_6$ and [3] $CuSb_2O_6$ unaffected by the onset of long-range magnetic order is likely caused by a different mechanism that remains to be determined.

ACKNOWLEDGMENTS

This material is based upon work supported by the U.S. Department of Energy (DOE), Office of Science Basic Energy Sciences (BES) under Awards No. DE-SC0008607 (Univ. Miami) and No. DE-SC0016156 (Montana St. Univ.).

[1] Y. Ando, J. Takeya, D. L. Sisson, S. G. Doettinger, I. Tanaka, R. S. Feigelson, and A. Kapitulnik, Phys. Rev. B **58**, R2913 (1998).

[2] M. Hofmann, T. Lorenz, G. S. Uhrig, H. Kierspel, O. Zabara, A. Freimuth, H. Kageyama, and Y. Ueda, Phys. Rev. Lett. **87**, 047202 (2001).

[3] N. Prasai, A. Rebello, A. B. Christian, J. J. Neumeier, and J. L. Cohn, Phys. Rev. B **91**, 054403 (2015).

[4] Byung-Gu Jeon, B. Koteswararao, C. B. Park, G. J. Shu, S. C. Riggs, E. G. Moon, S. B. Chung, F. C. Chou, and K. H. Kim, Sci. Rep. **6**, 36970 (2016).

[5] A. B. Christian, S. H. Masunaga, A. T. Schye, A. Rebello, J. J. Neumeier, and Y.-K. Yu, Phys. Rev. B **90**, 224423 (2014).

[6] A. B. Christian, A. Rebello, M. G. Smith, and J. J. Neumeier, Phys. Rev. B **92**, 174425 (2015).

[7] A. B. Christian, C. D. Hunt, and J. J. Neumeier, Phys. Rev. B **96**, 024433 (2017).

[8] A. B. Christian, A. T. Schye, K. O. White, and J. J. Neumeier, J. Phys.: Condens. Matter **30**, 195803 (2018).

[9] A. B. Christian, Magnetic and thermal properties of low-dimensional single-crystalline transition-metal antimonates and tantalates, Ph.D. thesis, Montana State University, 2017.

[10] D. T. Maimone, A. B. Christian, J. J. Neumeier, and E. Granado, Phys. Rev. B **97**, 104304 (2018).

[11] J. N. Reimers, J. E. Greedan, C. V. Stager, and R. Kremer, J. Solid State Chem. **83**, 20 (1989).

[12] R. K. Kremer and J. E. Greedan, J. Solid State Chem. **73**, 579 (1988).

[13] J. M. Law, H.-J. Koo, M.-H. Whangbo, E. Brücher, V. Pomjakushin, and R. K. Kremer, Phys. Rev. B **89**, 014423 (2014).

[14] D. Kasinathan, K. Koepernik, and H. Rosner, Phys. Rev. Lett. **100**, 237202 (2008).

[15] T. J. S. Munsie, M. N. Wilson, A. Millington, C. M. Thompson, R. Flacau, C. Ding, S. Guo, Z. Gong, A. A. Aczel, H. B. Cao, T. J. Williams, H. A. Dabkowska, F. Ning, J. E. Greedan, and G. M. Luke, Phys. Rev. B **96**, 144417 (2017).

[16] F. D. M. Haldane, Phys. Lett. A **93**, 464 (1983); Phys. Rev. Lett. **50**, 1153 (1983).

[17] I. Affleck, J. Phys.: Condens. Matter **1**, 3047 (1989).

[18] R. Berman, *Thermal Conduction in Solids* (Clarendon, Oxford, 1976).

[19] G. A. Slack, in *Solid State Physics*, edited by H. Ehrenreich, F. Seitz, and D. Turnbull (Academic, New York, 1979), Vol. 34, p. 1.

[20] F. W. Sheard and G. A. Toombs, Solid State Commun. **12**, 713 (1973).

[21] W. N. Wybourne, B. J. Kiff, D. N. Bachelder, D. Greig, and M. Sahota, J. Phys. C **18**, 309 (1985).

[22] A. V. Sologubenko, K. Giannò, H. R. Ott, A. Vietkine, and A. Revcolevschi, Phys. Rev. B **64**, 054412 (2001).

[23] J. G. Traylor, H. G. Smith, R. M. Nicklow, and M. K. Wilkinson, Phys. Rev. B **3**, 3457 (1971).

[24] F. Gervais and W. Kress, Phys. Rev. B **31**, 4809 (1985).

[25] V. I. Torgashev, V. B. Shirokov, A. S. Prokhorov, B. Gorshunov, P. Haas, M. Dressel, B. J. Gibson, R. K. Kremer, A. V. Prokofiev, and W. Assmus, Phys. Rev. B **67**, 134433 (2003).

[26] M. Schrade and T. G. Finstad, Phys. Status Solidi B 1800208 (2018).

[27] J. M. Law, H. Benner, and R. K. Kremer, J. Phys.: Condens. Matter **25**, 065601 (2013).

[28] J. des Cloizeaux and J. J. Pearson, Phys. Rev. **128**, 2131 (1962).

[29] I. A. Zaliznyak, S.-H. Lee, and S. V. Petrov, Phys. Rev. Lett. **87**, 017202 (2001).

[30] O. Golinelli, T. Jolicoeur, and R. Lacaze, J. Phys: Condens. Matter **5**, 1399 (1993).

[31] J. C. Wu, J. D. Song, Z. Y. Zhao, J. Shi, H. S. Xu, J. Y. Zhao, X. G. Liu, X. Zhao, and X. F. Sun, J. Phys.: Condens. Matter **28**, 056002 (2016).

[32] R. Hentrich, A. U. B. Wolter, X. Zotos, W. Brenig, D. Nowak, A. Isaeva, T. Doert, A. Banerjee, P. Lampen-Kelley, D. G. Mandrus, S. E. Nagler, J. Sears, Y.-J. Kim, B. Büchner, and C. Hess, Phys. Rev. Lett. **120**, 117204 (2018).

[33] M. Montagnese, M. Otter, X. Zotos, D. A. Fishman, N. Hlubek, O. Mityashkin, C. Hess, R. Saint-Martin, S. Singh, A. Revcolevschi, and P. H. M. van Loosdrecht, Phys. Rev. Lett. **110**, 147206 (2013).

[34] E. Husson, Y. Repelin, and H. Brusset, Spectrochim. Acta Part A **35**, 1177 (1979).

[35] D. T. Maimone, Ph.D. thesis, "Gleb Wataghin" Institute of Physics, University of Campinas, UNICAMP, Brazil, 2016.

[36] D. J. Lockwood and M. G. Cottam, J. Appl. Phys. **64**, 5876 (1988).

[37] E. Aytan, B. Debnath, F. Kargar, Y. Barlas, M. M. Lacerda, J. X. Li, R. K. Lake, J. Shi, and A. A. Balandin, Appl. Phys. Lett. **111**, 252402 (2017).